Pramana – J. Phys. (2017) 89:6
DOI 10.1007/s12043-017-1401-4

Magnetic interactions and electronic structure of $Pt_2Mn_{1-x}Y_xGa$ (Y = Cr and Fe) system: An *ab-initio* calculation

TUFAN ROY[1] and APARNA CHAKRABARTI[1,2,*]

[1]Homi Bhaba National Institute, Training School Complex, Anushakti Nagar, Mumbai 400 094, India
[2]Theory and Simulations Laboratory, Human Resources Development Section, Raja Ramanna Centre for Advanced Technology, Indore 452 013, India
*Corresponding author. E-mail: aparnachakrabarti@gmail.com

Published online 19 June 2017

Abstract. First-principles density functional theory-based calculations have been carried out to predict the effects of Mn replacement by Fe and Cr on electronic as well as magnetic properties of Pt_2MnGa and Ni_2MnGa. All the materials studied here are predicted to have conventional Heusler alloy structure in their ground state and they are found to be electronically stable on the basis of their respective formation energy. The replacement of Mn by Fe leads to a ferromagnetic ground state whereas in case of Mn replacement by Cr an intrasublattice antiferromagnetic configuration has been observed to have lower energy. We study the magnetic exchange interaction between the atoms for the materials with ferromagnetic and antiferromagnetic configurations to show the effects of Fe and Cr substitution at Mn site on the magnetic interactions of these systems. Detailed analysis of electronic structure in terms of density of states has been carried out to study the effect of substitution.

Keywords. Heusler alloy; martensitic transition; shape memory; density functional theory.

PACS Nos 71.15.Nc; 71.15.Mb; 81.30.Kf; 75.50.Cc

1. Introduction

Ni_2MnGa is one of the most studied magnetic shape memory alloys (MSMA). It shows magnetic field-induced strain (MFIS) and large magnetoresistance effect (MRE), which make Ni–Mn–Ga a suitable candidate for practical application as actuators and sensors [1–3]. The materials which are known as MSMA have two different crystal structures, a high-temperature phase with high crystal symmetry (cubic) known as austenitic phase and the low-temperature phase of lower symmetry (e.g. tetragonal, orthorhombic) known as martensitic phase. The temperature at which the structural transition occurs is known as martensitic transition temperature (T_M). For Ni_2MnGa, T_M is reported to be 210 K. Besides MFIS and MRE, the MSMAs are well known to show magnetocaloric effect (MCE) [4] and inverse magnetocaloric effect [5,6], which make them potential materials of choice in echofriendly refrigerator.

However, a major drawback of Ni_2MnGa is its low (less than room temperature) martensitic transition temperature and its brittleness. Therefore, the current challenge for the researchers is to find new materials which possess better mechanical property and preferably higher T_M and T_c (Curie temperature) compared to Ni_2MnGa. It is reported in literature that both T_M and T_c are highly composition-dependent. Experimentally, it has been observed that partial Cu substitution at the Mn site of Ni_2MnGa raises the martensitic transition temperature [7]. In our previous work [8], based on first-principles calculations, we have also shown that Cu substitution at Mn or Ga site improves the martensitic transition temperature whereas the Cu substitution at Ni site stabilizes the austenite phase more.

Recently, on the basis of first-principles calculations, 14% MFIS has been reported for $Ni_{1.75}Pt_{0.25}MnGa$ [9]. It has also been predicted that systematic as well as full substitution at Ni site by Pt improves the mechanical property as well as martensitic transition temperature [10,11]. In literature, it is reported that Mn replacement by Fe in Ni_2MnGa with suitable amount of substitution pushes T_M close to room temperature [12,13]. Keeping the goal in mind for searching for better Heusler alloys with higher T_M and T_c as well as lower inherent crystalline brittleness (ICB), we probed the replacement of Mn by Cr and Fe in our earlier work [11] and we have shown that full replacement

of Mn by Fe decreases the ICB in both Ni_2MnGa and Pt_2MnGa. There we have also reported significant increase of T_M with respect to parent materials. Now it will be interesting to probe how the electronic density of states as well as magnetic exchange interaction are modified in the case of Mn substitution by Fe and Cr. Therefore, here, on the basis of first-principles calculations, we study systematically the effect of Fe and Cr substitution at the Mn site on their electronic properties, as well as on T_M and T_c for Pt_2MnGa as well as Ni_2MnGa. Using spin-polarized fully relativistic Korringa–Kohn–Rostoker (SPRKKR) method, we also study the Heisenberg magnetic exchange coupling parameters to understand the effect of substitution on the magnetic interaction in these materials.

2. Method

For the first-principles calculation, geometry optimization of all the materials studied here have been performed using Viena ab initio simulation Package (VASP) [14] along with projected augmented wave method (PAW) [15]. Generalized gradient approximation (GGA) over local density approximation (LDA) of Perdew, Burke and Ernzerhof has been used for exchange correlation functional [16]. We use energy cut-off for plane wave 500 eV and convergence has been tested. The final energies have been calculated with a k-mesh of $15 \times 15 \times 15$ for the cubic case. The energy and force tolerance used were 10 μeV and 10 meV/Å, respectively.

We have performed relativistic spin-polarized all-electron calculation on optimized geometry to understand magnetic as well as electronic properties, that is, density of states (DOS). All the calculations have been carried out using full potential linearized augmented plane wave (FPLAPW) program [17], with the generalized gradient approximation for the exchange correlation functional [16]. Brillouin zone (BZ) integration has been carried out using the tetrahedron method with Bloechl corrections [17] to obtain the electronic properties. An energy cut-off for the plane-wave expansion of about 16 Ry is used and the charge density cut-off used here is $G_{max} = 14$. For cubic phase, the number of k points for the self-consistent field (SCF) cycles in the reducible (irreducible) BZ is about 8000 (220). The SCF calculations have been performed with 0.1 mRy as the tolerance for energy convergence per atom and charge convergence is set to 0.0001.

To probe the details of magnetic interaction between the atoms, calculation of Heisenberg exchange coupling constant J_{ij} has been carried out. SPRKKR program, provided by Ebert *et al* [18], has been used to calculate J_{ij} within a real space approach [19]. The exchange and correlation term has been incorporated within the GGA framework [16]. For SCF cycles, the number of k points has been taken as 1000. The angular momentum expansion up to $l_{max} = 3$ has been taken for each atom.

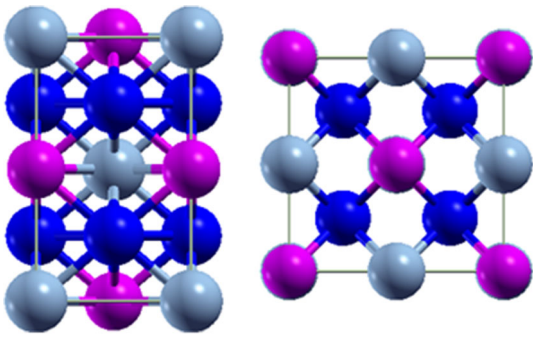

Figure 1. Structural model of tetragonal phase and cubic phase for X_2YZ system where X = Ni, Pt; Y = Cr, Mn, Fe; Z = Ga. Blue ball denotes X atom, grey ball denotes Y atom and magenta ball denotes Ga atom.

3. Results and discussions

3.1 *Electronic property*

From the total energy calculation it has been found that, for all these materials, parent as well as substituted ones, conventional Heusler alloy structure (figure 1) is energetically lower compared to their inverse Heusler alloy structure. We have analysed the variation of formation energy for all the materials as a function of Fe or Cr substitution in our previous work [11]. There we have also shown from the variation of energy as a function of tetragonal distortion and the observation of conservation of volume in both cubic and tetragonal phases, that all the materials in their ferromagnetic (FM) phase are likely to show tetragonal distortion leading to the possibility of a martensitic transition. In this work, we are interested to see the electronic density of states of the cubic austenite phase of the substituted alloys in detail.

First we discuss the DOS of the Ni_2YGa (Y = Cr, Mn, Fe) systems and compare these results with the Pt_2YGa systems. Figure 2 shows the total DOS of all Ni-based materials along with spin-polarized DOS. From the total DOS, we can see that for Ni_2MnGa there is a double peak structure very close to Fermi level. The implication of this peak has been discussed in detail in our previous work ([10] and references therein). In the case of Ni_2MnGa, Barman *et al* have shown that the peak in the minority DOS very close to Fermi level plays a crucial role in favouring martensitic transition [20].

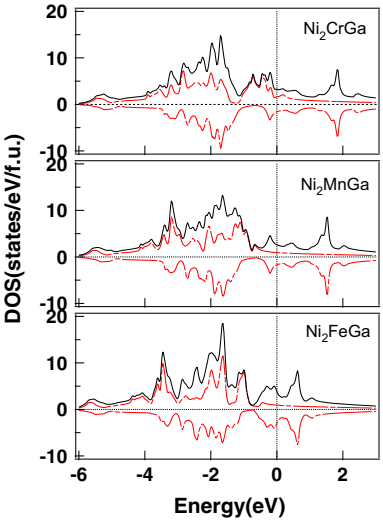

Figure 2. Total DOS and spin-polarized DOS for Ni-based materials; solid line represents the total DOS and the majority and minority DOS are shown by dash–dotted lines.

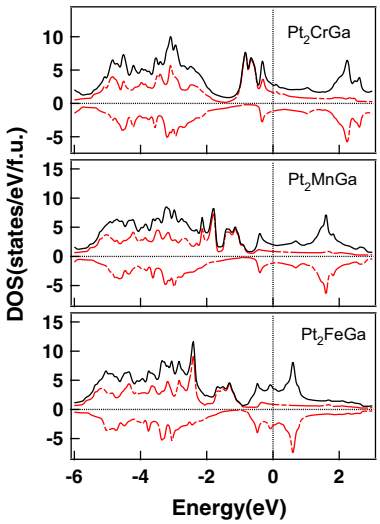

Figure 3. Total DOS and spin-polarized DOS for Pt-based materials; solid line represents the total DOS and the majority and minority DOS are shown by dash–dotted lines.

From figure 2, it is clear that all the Ni-based materials have a prominent Ni d-electron derived peak very close to (also below) the Fermi level. For Fe and Mn cases, the minority spin makes the major contribution, but in the case of Cr, both the spin densities of states show similar intensity. It is expected from their respective DOS that tetragonal distortion may lower the energy of these systems compared to their cubic structure, which can be very well explained by band Jahn–Teller distortion mechanism as has been observed in the case of Ni_2MnGa in [20,21].

Similarly, for Pt-based systems also, from figure 3, we can find such peaks in the DOS very close to Fermi level; this observation favours the possibility of martensitic transition. It is interesting to observe that the contribution of the majority and minority spin in this feature of the DOS close to Fermi level is similar in both Pt and Ni-based systems.

To understand the electronic structure of the Pt-based materials in greater details, the partial DOSs are plotted in figure 4. From the partial DOS of the Pt_2MnGa and Pt_2FeGa, it is seen that the separation of majority and minority DOS for Mn and Fe, respectively, is clear and complete. We observe that for Pt_2YGa (Y = Mn, Fe), the occupied DOS of the Y atom is dominated by the majority spin and the respective unoccupied DOS is dominated by the minority spin. For Pt_2MnGa, majority DOS of the Mn atom is centred around -1.242 eV whereas the respective minority DOS is centred around 1.588 eV. For Pt_2FeGa, the majority DOS of the Fe atom is centred around -1.505 eV and respective minority DOS is centred around 0.617 eV. This gives the idea of a large exchange splitting in the case of Y atom in both Pt_2MnGa and Pt_2FeGa, which is evidently more

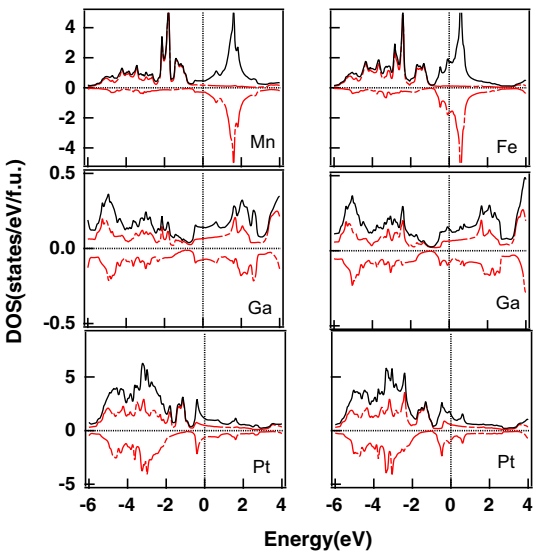

Figure 4. Partial spin-polarized DOS for Pt-based materials.

for the Mn atom. This large exchange splitting of Y atom for both the compounds leads to large partial magnetic moments on the Y atom ($3.671\mu_B$ for Mn in Pt_2MnGa, $3.025\mu_B$ for Fe in Pt_2FeGa) in both the materials [11]. On the contrary, for the Pt atom, in both cases (figure 4), the majority and minority DOSs are very similar in peak position and intensity in the occupied region, leading to a much lower partial moment of the Pt atom ($0.138\mu_B$ in Pt_2MnGa, $0.088\mu_B$ in Pt_2FeGa) [11]. For both Pt_2MnGa and Pt_2FeGa, there is significant hybridization between Ga 4p and outermost d electrons of the Pt atom and a double peak structure around Fermi level is observed which plays a crucial role in the stability of these materials. This observation is similar to our earlier work [10].

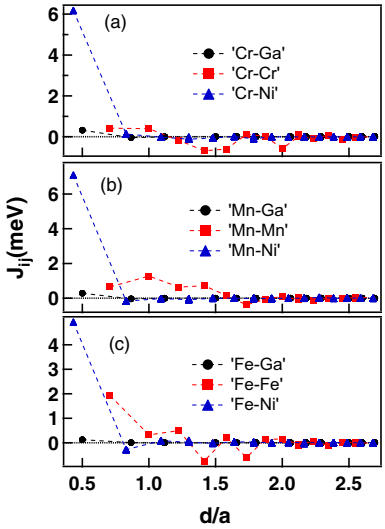

Figure 5. Heisenberg exchange parameters J_{ij} of Y atom (Y = Cr, Mn, Fe) with all the atoms as a function of normalized distance d/a, where a is the lattice constant of the austenitic phase for (**a**) Ni_2CrGa, (**b**) Ni_2MnGa and (**c**) Ni_2FeGa.

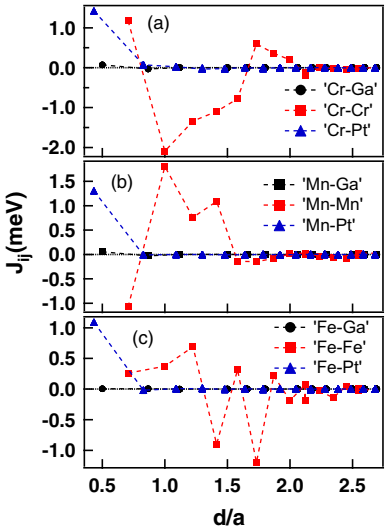

Figure 6. Heisenberg exchange parameters J_{ij} of Y atom (Y = Cr, Mn, Fe) with all the atoms as a function of normalized distance d/a, where a is the lattice constant of the austenitic phase for (**a**) Pt_2CrGa, (**b**) Pt_2MnGa and (**c**) Pt_2FeGa.

3.2 *Magnetic interaction*

In the literature, it is well established that Ni_2MnGa possesses ferromagnetic ground-state configuration. For Pt_2MnGa, some studies suggest [9,10,22] that it has ferromagnetic ground state. Therefore, we start the calculations for the substituted materials where Mn is replaced by Fe and Cr, by considering them as ferromagnetic in nature. The total magnetic moments of these materials along with partial moments are reported in detail in our previous work [11]. We observed that for Pt-based systems, more localization of Mn-magnetic moment is expected compared to Ni-based systems because of the larger Mn–Mn separation in the former. To get detailed insight of the magnetic interaction, in this work, we study the Heisenberg exchange coupling constants for all the materials in their cubic austenite phase. These coupling parameters give indication about the nature of predominant magnetic interactions between different atoms present in the materials.

The calculations of J_{ij} are performed within a cluster of radius $3a$, where a is the optimized lattice parameter of the respective unit cell. To start with, we present the Heisenberg coupling parameters for the Ni-based systems in figure 5. This figure suggests that for all the Ni-based materials, the X–Y (X = Ni; Y = Cr, Mn, Fe) interaction is purely ferromagnetic in nature. As X and Y atoms are nearest neighbours, direct interaction between these atoms becomes dominating, and it vanishes at larger distances. For all the cases, Y–Ga interaction is very weak, and so we do not discuss this in further analysis of our results. Now we move our focus to the Y–Y interaction: we find that in Ni_2MnGa, this interaction is ferromagnetic up to the fifth coordination shell, which is well supported by [8] and it is RKKY-type of interaction [23] in nature. However, for Ni_2FeGa, we find that the interaction becomes oscillatory which clearly indicates the presence of a RKKY-type of interaction [23] in the system. Similar is the case for the Cr atom, as is observed in the case of Ni_2CrGa.

Figure 6 also suggests that similar to the Ni-based materials, the X–Y (X = Pt; Y = Cr, Mn, Fe) interaction is purely ferromagnetic and it almost vanishes after the first nearest-neighbour interaction. In the case of Pt_2FeGa, Fe–Fe interaction is very similar to that of Ni_2FeGa. But for Pt_2MnGa here, the first Mn–Mn interaction is strongly antiferromagnetic while the third, fourth and fifth Mn–Mn interactions are strongly ferromagnetic. From the J_{ij} plot of Pt_2CrGa, it is clear that Cr–Cr interaction is more of antiferromagnetic type, as is observed from figure 6, though the first-neighbour interaction has a ferromagnetic nature.

In figure 7, we plot the T_M values from our previous calculations [11]. In figure 7, we also present the Curie temperature (T_c) for all the materials in the FM state, calculated from the corresponding J_{ij} values under a mean-field approximation following the approach of Meinert *et al* [24]. Both the temperature values show a systematic change as the composition is changed. We note that the experimental T_c of Ni_2MnGa is 363 K [25]. It is already reported in literature that mean-field approximation overestimates T_c [26]. It is observed that Ni_2CrGa among the Ni-based materials and Pt_2CrGa among the Pt-based materials possess the lowest

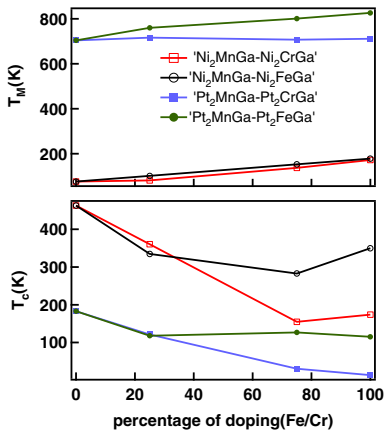

Figure 7. Curie temperature (T_c) and martensite temperature (T_M) as a function of substitution.

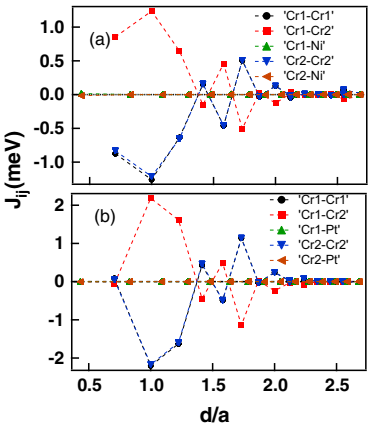

Figure 8. Heisenberg exchange parameters J_{ij} of Cr atom with its neighbours as a function of the normalized distance d/a, where a is the lattice constant of the austenitic phase for (**a**) Ni_2CrGa and (**b**) Pt_2CrGa in their correct magnetic ground state (AFM) configuration.

ferromagnetic transition temperature (T_c). One possible reason behind this may be the presence of antiferromagnetic (AFM) type exchange interaction between Cr–Cr for both of them.

3.2.1 *Antiferromagnetic interaction in Cr-based systems.* There is an indication of the presence of antiferromagnetic interaction in the Cr-based materials as is seen from figures 5, 6 and 7. It is known that both Cr and Mn have antiferromagnetic interactions in their bulk form. From the Bethe–Slater curve, it is clear that Cr has stronger antiferromagnetic J_{ij} interaction compared to Mn. We also note that, Sharma *et al* [27] reported that the doping of Cr at the Mn site of Ni–Mn–In reduces the FM interaction, while doping by Fe leads to an increase of FM interaction. All these observations have motivated us to probe the possibility of antiferromagnetic ground state in Ni_2CrGa and Pt_2CrGa in our earlier work [11]. In that work, we have predicted that the true ground-state magnetic configuration for Ni_2CrGa and Pt_2CrGa is an intrasublattice AFM configuration.

In figure 7, we show the variation of J_{ij} in their magnetic ground state (AFM configuration) of Ni_2CrGa and Pt_2CrGa. The calculations for intrasublattice AFM configuration have been performed within coherent potential approximation implemented in SPRKKR code, by considering that 50% of the body-centred site (fractional coordinates 0.5, 0.5, 0.5) is occupied by up-spin Cr atom (Cr1) and the rest of the site is occupied by down-spin Cr atom (Cr2). From figure 8, as expected, we can see that Cr1–Cr1 interaction is almost identical with Cr2–Cr2 interaction for the materials. Also, the interaction is of RKKY-type as is seen from the J_{ij} plots. One more interesting point for both the systems is that the magnetic interaction between Cr1–Cr1 (also Cr2–Cr2) is exactly cancelled by the Cr1–Cr2 (Cr2–Cr1) interaction. These two strong mutually cancelling exchange interactions may have led to the antiferromagnetic ground-state magnetic configuration for both these systems.

4. Conclusion

Using first-principles density functional theory, we have discussed the effects of Mn replacement by Fe and Cr in the case of Pt_2MnGa as well as Ni_2MnGa on the respective electronic density of states as well as magnetic interaction. It is clear that all the Ni and Pt-based materials have prominent Ni and Pt d-electron derived peaks, respectively, very close to (also below) the Fermi level. It is expected from their respective DOS that tetragonal distortion may lower the energy of these systems compared to their cubic structure, which can be very well explained by band Jahn–Teller distortion mechanism. Further, while for Fe and Mn cases, the minority spin makes the major contribution, in the case of Cr, both the spin densities of states show similar intensity. The total and partial spin-polarized DOS as well as the valence band width show similarity between the Pt and Ni-based alloys.

The plots of J_{ij} as a function of normalized interneighbour spacing suggest that in all the materials the X–Y interaction (X = Pt, Ni; Y = Cr, Mn, Fe) has a direct ferromagnetic interaction. But Y–Y (Y = Cr, Mn, Fe) interaction is mainly RKKY-type for both Fe-based systems, i.e. Ni_2FeGa and Pt_2FeGa. For Ni_2MnGa also, the Mn–Mn interaction is RKKY-type, with a ferromagnetic interaction upto the fifth nearest neighbour. On the contrary, in Pt_2MnGa the antiferromagntic interaction becomes somewhat dominating between Mn–Mn, though an overall ferromagnetic state is energetically

lower compared to the antiferromagnetic state. But in the case of Cr substitution at Mn site, in both Ni_2CrGa and Pt_2CrGa, Cr–Cr antiferromanetic exchange interaction becomes predominant over the ferromagnetic one, leading to an intrasublattice antiferromagnetic configuration in their respective ground state [11] and the J_{ij} plots for the AFM phase show interesting difference with the corresponding plots of the ferromagnetic configuration of the Cr-based alloys.

Acknowledgements

Authors thank P D Gupta and P A Naik for facilities and encouragement throughout the work. The scientific computing group, computer centre of RRCAT, Indore and P Thander are thanked for help in installing and support in running the codes. S R Barman and C Kamal are thanked for useful discussions. TR thanks HBNI, RRCAT for financial support.

References

[1] P J Webster, K R A Ziebeck, S L Town and M S Peak, *Philos. Mag. B* **49**, 295 (1984)
[2] C Biswas, R Rawat and S R Barman, *Appl. Phys. Lett.* **86**, 202508 (2005)
[3] A Sozinov, A A Likhachev, N Lanska and K Ullakko, *Appl. Phys. Lett.* **80**, 1746 (2002)
[4] F X Hu, B Shen and J Sun, *Appl. Phys. Lett.* **76**, 3460 (2000)
[5] T Krenke, E Duman, M Acet, E F Wassermann, X Moya, L Manosa and A Planes, *Nat. Mater.* **4**, 450 (2005)
[6] R Kainuma, Y Imano, W Ito, Y Sutou, H Morito, H Okamato, S Kitakami, O Oikawa, A Fujita, T Kanomata and K Isida, *Nature (London)* **439**, 957 (2006)
[7] S Roy, E Blackburn, S M Valvidares, M R Fitzsimmons, S C Vogel, M Khan, I Dubenko, S Stadler, N Ali, S K Sinha and J B Kortright, *Phys. Rev. B* **79**, 235127 (2009)
[8] A Chakrabarti, M Siewert, T Roy, K Mondal, A Banerjee, M E Gruner and P Entel, *Phys. Rev. B* **88**, 174116 (2013) and references therein
[9] M Siewert, M E Gruner, A Dannenberg, A Chakrabarti, H C Herper, M Wuttig, S R Barman, S Singh, A Al-Zubi, T Hickel, J Neugebauer, M Gillessen, R Dronskowski and P Entel, *Appl. Phys. Lett.* **99**, 191904 (2011)
[10] T Roy, M E Gruner, P Entel and A Chakrabarti, *J. Alloys Compd.* **632**, 822 (2015)
[11] T Roy and A Chakrabarti, *J. Magn. Magn. Mater.* **401**, 929 (2016)
[12] K Oikawa, T Ota, T Ohmori, Y Tanaka, H Morito, A Fijita, R Kainuma, K Fukamichi and K Ishida, *Appl. Phys. Lett.* **81**, 5201 (2002)
[13] H R Zhang, C Ma, H F Tian, G H Wu and J Q Li, *Phys. Rev. B* **77**, 214106 (2008)
[14] G Kresse and J Furthmuller, *Phys. Rev. B* **54**, 11169, (1996); G Kresse and D Joubert, *Phys. Rev. B* **59**, 1758 (1999), VASP 5.2 program package is fully integrated in the MedeA platform (Materials Design, Inc.) with a graphical user interface enabling the computation of the properties
[15] P E Blochl, *Phys. Rev. B* **50**, 17953 (1994)
[16] J P Perdew, K Burke and M Ernzerhof, *Phys. Rev. Lett.* **77**, 3865 (1996)
[17] P Blaha, K Schwartz, G K H Madsen, D Kvasnicka and J Luitz, *WIEN2K, An augmented plane wave plus local orbitals program for calculating crystal properties* (Karlheinz Schwarz, Tech Universitaet, Wien, Austria, 2002), ISBN: 3-9501031-1-2
[18] H Ebert, D Kodderitzsch and J Minar, *Rep. Prog. Phys.* **74**, 096501 (2011)
[19] A I Liechtenstein, M I Katsnelson, V P Antropov and V A Gubanov, *J. Magn. Magn. Mater.* **67**, 65 (1987)
[20] S R Barman, S Banik and A Chakrabarti, *Phys. Rev. B* **72**, 184410 (2005) and references therein
[21] T Roy, D Pandey and A Chakrabarti, *Phys. Rev. B* **93**, 184102 (2016)
[22] Antje Dannenberg, *Ab initio and Monte Carlo investigations of structural, electronic and magnetic properties of new ferromagnetic Heusler alloys with high Curie temperatures*, Ph.D. thesis (University of Duisburg-Essen, 2011)
[23] M A Ruderman and C Kittel, *Phys. Rev.* **96**, 99 (1954); T Kasuya, *Prog. Theor. Phys.* **16**, 45 (1956); K Yosida, *Phys. Rev.* **106**, 893 (1957)
[24] M Meinert, J M Schmalhorst and G Reiss, *J. Phys.: Condens. Matter* **23**, 036001 (2011); M Meinert, J M Schmalhorst and G Reiss, *J. Phys.: Condens. Matter* **23**, 115005 (2011) and the references therein
[25] H Nishihara, K Komiyama, I Oguro, T Kanomata and V Chernenko, *J. Alloys Compd.* **442**, 191 (2007)
[26] M Pajda, J Kudrnovsky, I Turek, V Drchal and P Bruno, *Phys. Rev. B* **64**, 174402 (2001)
[27] V K Sharma, M K Chattopadhyay, S K Nath, K J S Sokhey, R Kumar, P Tiwari and S B Roy, *J. Phys.: Condens. Matter* **22**, 486007 (2010)